nature water

Article

https://doi.org/10.1038/s44221-023-00126-0

Balancing-oriented hydropower operation makes the clean energy transition more affordable and simultaneously boosts water security

Received: 30 November 2022

Accepted: 2 August 2023

Published online: 18 September 2023

Check for updates

Zhanwei Liu & Xiaogang He

Reservoir hydropower offers a compelling combination of stability and flexibility services for modern water and power grids. However, its operating flexibility is poorly characterized in energy system planning, missing opportunities to cost-effectively uptake variable renewable energy (VRE) for a clean energy transition. In this study, we have developed a fully coupled reservoir operation and energy expansion model to quantify the economic and environmental benefits attained from adaptive hydropower operation in a high VRE future. Our case study of the China Southern Power Grid reveals that, in a 2050 net-zero grid, simply adapting hydropower operations to balance VRE can reduce 2018–2050 total system costs by 7% (that is, US$28.2 billion) and simultaneously save 123.8 km^3 of water each year (that is, more than three times the reservoir capacity of the Three Gorges Dam). These vast, yet overlooked, cost- and water-saving potentials highlight the importance of incorporating balancing-oriented hydropower operation into future pathways to jointly decarbonize and secure power and water grids.

The decarbonization of power systems is crucial to mitigate climate change[1] and requires a high penetration of variable renewable energy (VRE; mainly solar photovoltaic (PV) and wind power) to displace carbon-emitting electricity (for example, coal- and gas-fired power). Yet, the generation of weather-dependent VRE is unlikely to align with the timing of grid demand due to the intermittent, fluctuating and stochastic nature of weather systems[2]. In a high VRE power system, it is therefore crucial to deploy diverse and flexible technologies[3] to increase grid flexibility so that a reliable and resilient power supply can be ensured. Among the many alternative flexible options, reservoir hydropower is by far the most mature and the largest grid-connected clean technology[4]. It not only supplies carbon-free and cost-competitive energy, but also delivers vital flexibility services that can facilitate the low-carbon transition, characterized by its short start-up and shut-down time, quick ramping speed, low operation costs and long-duration (for example, interseasonal or interannual) energy buffering capabilities[5]. Globally, hydropower alone supplies 4,252 TWh of electricity, accounting for 17% of the total electricity consumed in 2021. Hydropower also contributes nearly one-third (29%) of global flexibility services measured by hourly ramping needs[6].

Reservoir hydropower plays a versatile role in safeguarding both power and water grids (that is, complex cascade reservoirs connected by river networks) owing to its generational flexibility and storage services[7]. Yet, conventional hydropower operations are being used to minimize load demand fluctuations[8]. These hydropower operations were designed on the basis of historical conditions when VRE did not represent a large share of electricity generation. In a rapidly evolving power grid with a growing penetration of VRE, such outdated operations could

Department of Civil and Environmental Engineering, College of Design and Engineering, National University of Singapore, Singapore, Singapore.
e-mail: hexg@nus.edu.sg

miss the opportunity to fully tap the potential of flexible hydropower to support VRE integration[2,9]. They could also unintentionally increase the vulnerability of power[10] and water[11] grids, especially under climate shocks. For instance, low reservoir inflows during prolonged droughts exacerbate water allocation trade-offs between hydropower production, agricultural supply and environmental flow requirements[12]. In addition to these sectoral water-use trade-offs, increased hydroclimate variability also heightens intertemporal trade-offs between storing water to enhance long-term drought resilience and releasing water to mitigate short-term flood risks[13]. There remain great, yet underexplored, opportunities[12] to minimize these trade-offs by leveraging the large-scale flexibility of hydropower and the rapid growth of VRE. This can be achieved by shifting reservoir operations from a conventional peak-shaving-oriented operation scheme[9], which is load demand-oriented and unable to adapt to a changing power mix, to a balancing-oriented hydropower operation that supports VRE integration and is well suited to adapt to changing temporal dynamics of electricity supply. However, it remains unclear to what extent adaptive hydropower operation can support the cost-effective integration of VRE and how VRE contributes to water sustainability.

A growing number of modelling studies[2,9,12,14–18] have investigated the spatiotemporal complementarity between VRE and hydropower in a power mix with an increasing share of VRE. However, most of these studies were conducted in silos, either focusing on the energy sector[2,9,14–16] or on the water sector[12,17]. A multi-benefit assessment of balancing-oriented hydropower operation accounting for the non-linear and dynamic nature of water–energy interactions is still lacking, especially for benefits related to water sustainability. This is hampered by a lack of modelling capabilities in existing energy expansion models to fully account for hydropower flexibility, which requires high spatial (both plant-level reservoir characteristics and regional-level reservoir cascade typologies), temporal (hourly to daily) and process (for example, generation flow variability, water head dynamics and power dispatch) resolutions (see Methods for details). Inadequate representation of hydropower flexibility can lead to over-investment in alternative flexible energy (for example, pumped storage hydropower and lithium-ion batteries) and therefore miss the opportunity to cost-effectively decarbonize power grids in an environmentally friendly manner. In this study, we developed an energy expansion model called **P**athways for **R**enewable **E**nergy **P**lanning coupling **S**hort-term **H**ydropower **O**pera**T**ion (PREP-SHOT; Supplementary Fig. 1) with explicit representation of hydropower flexibility to jointly optimize long-term investment and short-term operational decisions at the lowest cost (see Methods for details). We used PREP-SHOT to quantify the benefits of adaptive hydropower reoperations by comparing two operation schemes: 'FixedHydro' (conventional peak-shaving-oriented operations to maximize hydropower generation) and 'AdaptiveHydro' (balancing-oriented operations to compensate for the intermittency of VRE to minimize total system cost; see Methods for details).

We investigated the impact of balancing-oriented hydropower operation on energy expansion through a case study focusing on a renewable-dominated power grid, the China Southern Power Grid (CSG; Fig. 1a), where hydropower and VRE shared 40% of total power supplies in 2020 and will increase to 90% of the projected total load demand in 2050[19] (Fig. 1b). We designed 81 plausible carbon emission reduction scenarios (Fig. 1c) to represent uncertain decarbonization policies. We found that shifting reservoir operations from FixedHydro to AdaptiveHydro reduces the total system-wide cost over the period 2018–2050 by 7.1% if the CSG is fully decarbonized in 2050. Such cost savings are largely driven by the decline in curtailment rate of VRE supported by adaptive hydropower operations. Moreover, we estimated that a 1 MWh increase in VRE can save 320.0 m^3 of water each year under normal inflow conditions if short-term hydropower operations are jointly optimized with long-term energy expansion. This overlooked water-saving potential implies that a diversification of the power mix towards more VRE to reduce hydropower dependency has co-benefits that can simultaneously enhance the resilience of water grids to withstand future climate shocks. While our analysis focuses on China, PREP-SHOT and the quantitative assessment framework can be readily applied to other regions to design optimal energy decarbonization expansion pathways and guide sustainable water management.

Balancing-oriented hydropower operation reduces system costs

We found that balancing-oriented hydropower operation (AdaptiveHydro) can substantially reduce the total energy system cost compared with peak-shaving-oriented hydropower operation (FixedHydro) if the short-term operation of hydropower is jointly optimized with long-term energy expansion (Fig. 2a). Total cost reductions ($= \text{cost}^{\text{total}}_{\text{FixedHydro}} - \text{cost}^{\text{total}}_{\text{AdaptiveHydro}}$) increase almost linearly with carbon emission reduction targets, despite the non-linear increase in the total system-wide cost (Fig. 2a,b). With a 20% cut in 2050 carbon emissions from the 2018 levels, the 2018–2050 total system-wide cost of AdaptiveHydro (US$341.5 billion) is US$14.6 billion less than that of FixedHydro (US$356.1 billion), a 4.1% reduction. Such cost savings almost double to US$28.2 billion if carbon emissions are cut by 100% (Fig. 2a).

The attained cost savings are mainly driven by the reduced investment cost of VRE (that is, a 63% reduction in wind investment cost, although a 40% increase in solar investment cost) and the lower fuel cost of coal-fired plants (42% reduction in fuel cost), which, in total, make up ~65% of the total cost savings supported by adaptive hydropower operation (Fig. 2b). With the enhanced operational flexibility delivered by AdaptiveHydro compared with FixedHydro, a larger investment in solar is prioritized over wind (Supplementary Fig. 3a,b,e,f) given the lower cost of solar (Supplementary Table 2), despite its more fluctuating nature (sharp rise in the morning and sharp fall at dusk; Supplementary Figs. 3 and 4). Although the investment cost of solar is higher in AdaptiveHydro than in FixedHydro (Supplementary Fig. 3j), the combined investment cost of VRE (both solar and wind) in AdaptiveHydro is much lower (Fig. 2b and Supplementary Fig. 3i,j). This is mainly driven by the enhanced integration of VRE, as evidenced by the reduced curtailment rate of VRE (0.7–3.8% lower in AdaptiveHydro, depending on the level of decarbonization, Fig. 2c). Such elevated VRE generation in the power mix displaces more coal-fired generation, thus substantially reducing the cost of fuel for coal-fired power (US$6.2–11.1 billion, Fig. 2b).

The total cost savings from adaptive hydropower operations also depend on inflow variability, with consistently higher benefits in dry years than in wet years regardless of the decarbonization level (Fig. 2d). For a zero-carbon grid in 2050, an additional US$0.7 billion can be saved during dry years (US$28.8 billion, median estimate) compared with a normal year (US$28.1 billion). The total savings would, however, diminish to US$24.1 billion in scenarios with wetter inflow conditions, and these are associated with higher uncertainties (US$20.0–28.4 billion, 95th percentile range). Additionally, if the interannual variability of inflow is considered, the median estimate of such cost savings would further decline by 34.0%, 32.4% and 21.2% compared with dry, normal and wet years, respectively, under a zero-carbon grid in 2050 (Fig. 2d). According to our previous analysis (Fig. 2a,c), because a higher curtailment reduction of VRE is associated with higher cost savings, the reduced difference in the median VRE curtailment rate between FixedHydro and AdaptiveHydro (Supplementary Fig. 5a) explains why lower cost savings are obtained after considering the inflow interannual variability. The lower VRE curtailment reduction (Supplementary Fig. 5a) in interannual variability scenarios is mainly due to systematic seasonal biases between observed and simulated inflows (Supplementary Fig. 5b) over the representative periods, which leads to a biased yet heightened seasonal complementarity between hydro and VRE (Supplementary Fig. 5c,d).

https://doi.org/10.1038/s44221-023-00126-0

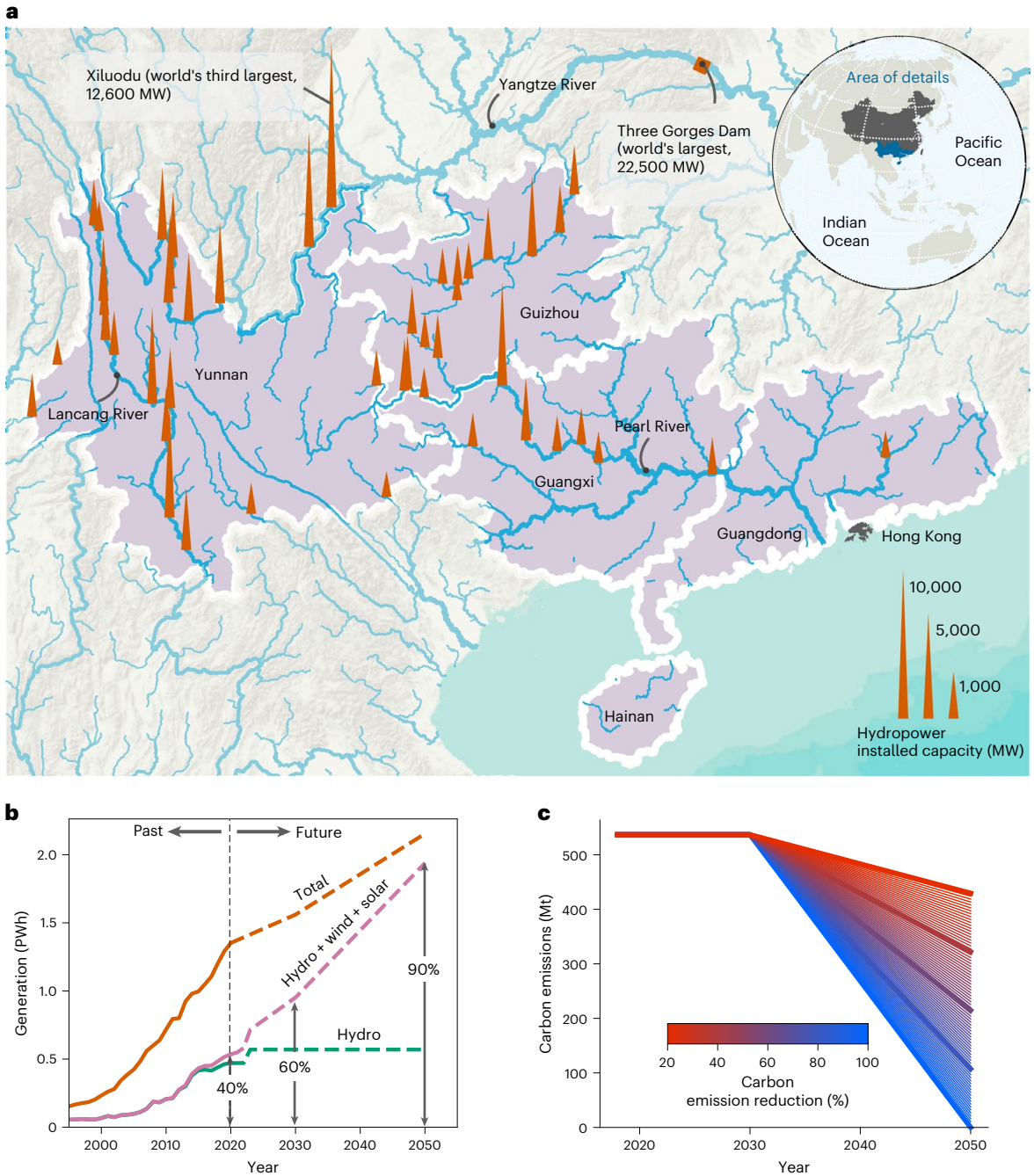

Fig. 1 | A renewable-dominated regional power grid in southwest China with ambitious decarbonization targets. a, Locations and installed capacity of 46 large hydropower stations (installed capacity exceeding 300 MW) in the CSG (see Supplementary Table 1 for plant-level details and Supplementary Fig. 2 for a detailed topology). Blue lines indicate major rivers; purple areas represent the five provinces (Guangdong, Guangxi, Guizhou, Yunnan and Hainan) in the CSG. The height of the spikes represents the installed capacity of each hydropower station. **b**, Previous and future energy generation portfolios of the CSG. The total renewable generation (including hydropower, solar PV and wind power) accounts for around 40%, 60% and 90% of the total power supplies in 2020, 2030 and 2050, respectively. **c**, Carbon emissions under different reduction scenarios. Each thin line represents the upper bound of a carbon dioxide emission reduction scenario. The five bold lines (from top to bottom) represent scenarios with 20%, 40%, 60%, 80% and 100% reductions in carbon emissions in 2050 relative to 2018 levels.

Increased VRE penetration boosts water security

We found that high VRE penetration can deliver additional non-monetary benefits that mitigate water use conflicts and enhance water availability beyond VRE's traditional role of decarbonization (Fig. 3a). In a high renewable energy system, increased VRE generation supported by reservoir hydropower and energy storage (for example, pumped storage hydropower, Fig. 3b) not only reduces the power grid's reliance on hydropower production (Fig. 3a and Supplementary Fig. 6e–h), but also increases the operational water head of hydropower stations (Supplementary Fig. 7).

We further quantified the water sustainability value (WSV) of VRE and examined how it varies with inflow conditions (Fig. 3c,d). The WSV measures how much water can be saved per megawatt hour power generation from VRE facilitated by AdaptiveHydro (empirically, the WSV is the slope of the dashed lines in Fig. 3c, see Methods for details). In a deeply decarbonized world (carbon emissions are cut by 80–100%

https://doi.org/10.1038/s44221-023-00126-0

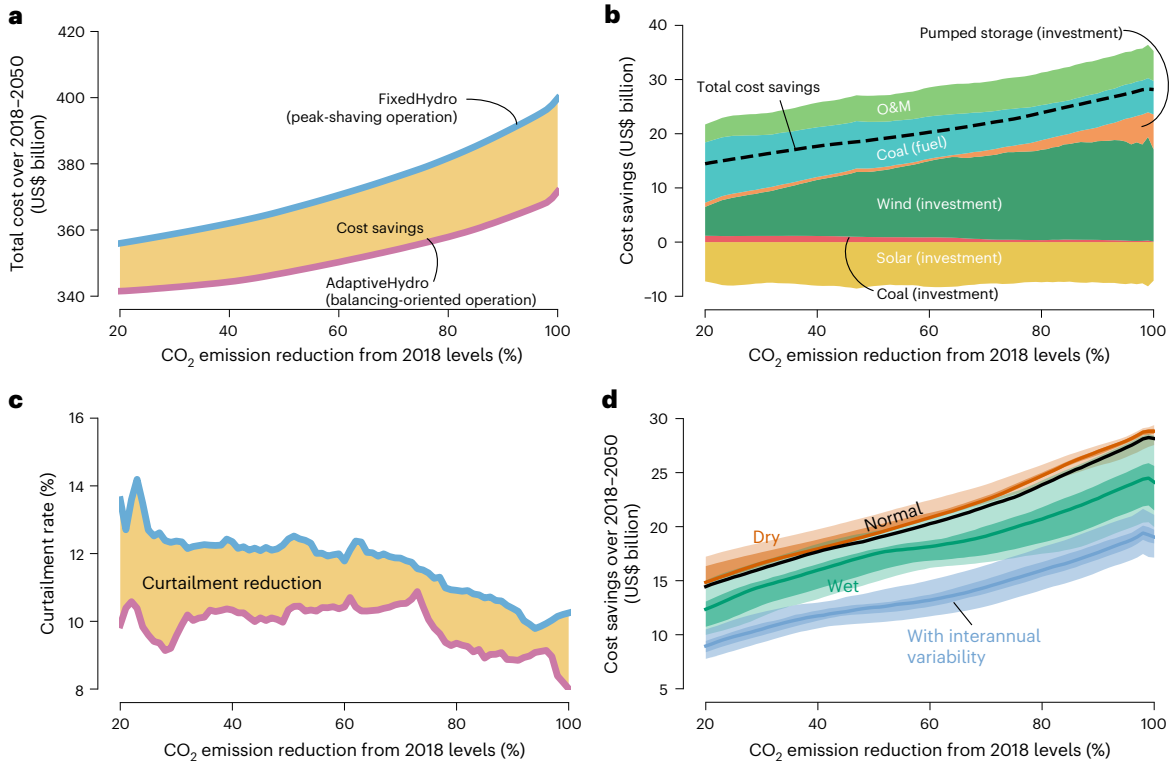

Fig. 2 | AdaptiveHydro operation reduces system costs. The AdaptiveHydro scheme reduces total system-wide cost and lowers the curtailment rate of VRE compared with FixedHydro. Such cost savings are driven by AdaptiveHydro and increase with decarbonization effort. **a**, Total system-wide costs over the entire planning horizon (2018–2050) under FixedHydro and AdaptiveHydro and the corresponding cost savings (yellow area) across different carbon emission reduction targets. **b**, Decomposition of total cost savings into six categories (that is, investment cost savings of coal-fired plant, investment cost savings of solar, investment cost savings of wind, investment cost savings of pumped storage hydropower, fuel cost savings of coal-fired plants and cost savings of operation and maintenance (O&M)) and how each category varies with the level of decarbonization. Negative cost savings indicate that the cost of a particular technology in the AdaptiveHydro scheme is greater than that of FixedHydro, as is the case with solar power. **c**, Curtailment reduction (yellow area) of VRE under AdaptiveHydro operation (pink line) compared with FixedHydro operation (blue line) across different decarbonization scenarios. **d**, Median (bold lines) and uncertainties (shading) of total cost savings under normal, dry ($n = 8$) and wet ($n = 8$) inflow conditions, as well as inflow conditions with interannual variability ($n = 100$) across different carbon emission reduction targets. The light and dark shading represent 95% and 50% confidence intervals, respectively.

in 2050 relative to 2018 levels), we found that a 1 MWh increase in VRE leads to annual water savings of ~320.0 m^3 under normal inflow conditions if the VRE is balanced by adaptive hydropower operations. The estimated WSV in wet years is considerably higher than the WSV in dry years, but the difference narrows as carbon emission reduction targets become more ambitious (Fig. 3d). For instance, with low decarbonization targets, the median WSV (across all inflow scenarios in the range) declines by 238.1 m^3 MWh^{-1}, an 82.0% decrease from 290.5 m^3 MWh^{-1} in wet years compared with 52.4 m^3 MWh^{-1} in dry years. This difference decreases to 148.5 m^3 MWh^{-1}, a 31.3% reduction in the WSV in wet years (473.9 m^3 MWh^{-1}) compared with that in dry years (325.4 m^3 MWh^{-1}), when a high carbon emission reduction target is achieved. Furthermore, the response of the WSV to inflow variability is less sensitive in dry years than in wet years. The variation in the WSV in dry years spans 58.0 m^3 MWh^{-1} across the high carbon emission reduction scenarios (95% range of 306.8–364.8 m^3 MWh^{-1}), which almost quadruples to 217.0 m^3 MWh^{-1} (95% range of 386.8–603.8 m^3 MWh^{-1}) in wet years, despite the substantial increase in the absolute magnitude of the WSV.

In addition to the sensitivity analysis of the WSV to inflow changes in dry and wet years, we also analysed how the interannual variability of inflow affects WSV estimates. Unlike the response of cost savings to interannual variability (Fig. 2d), we did not find any consistent patterns in the WSV after accounting for inflow interannual variability (Fig. 3d). The estimated WSV range considering interannual variability falls between the WSV ranges for dry and wet years, except in the case of the high decarbonization targets. These findings suggest that the effects of inflow interannual variability on WSV are more complex than its impact on cost savings.

Discussion

Hydropower-driven flexibility plays a crucial role in supporting VRE uptake towards power system decarbonization. Yet, its monetary and environmental value remains poorly characterized, especially in a high VRE future with uncertain decarbonization policies. Research on hydro–VRE complementarity traditionally has focused on economic dispatch[20]. In this study, we shifted the focus to jointly considering short-term economic dispatch with long-term energy expansion. This was aided by the new features of PREP-SHOT, which explicitly implements a two-way coupling of long-term energy expansion and short-term hydropower operation and therefore allows a more accurate quantification of total system cost and water sustainability. We found high, but overlooked, cost-saving (Fig. 2a), water-saving (Fig. 3a) and carbon abatement potential (see discussion below) if hydropower operations can be simply shifted from peak-shaving-oriented operation (with fixed and archaic operations) to balancing-oriented operation (with flexible and adaptive operations). Our results also show the value of AdaptiveHydro to be 'path-dependent' (Figs. 2a and 3d): earlier and deeper decarbonization allows the water sustainability benefits of VRE to be reaped to a larger extent.

Cost and water savings driven by increased penetration of hydro-compensated VRE can be explained by two intertwined mechanisms: volume effects and timing effects. Volume effects refer to more VRE

https://doi.org/10.1038/s44221-023-00126-0

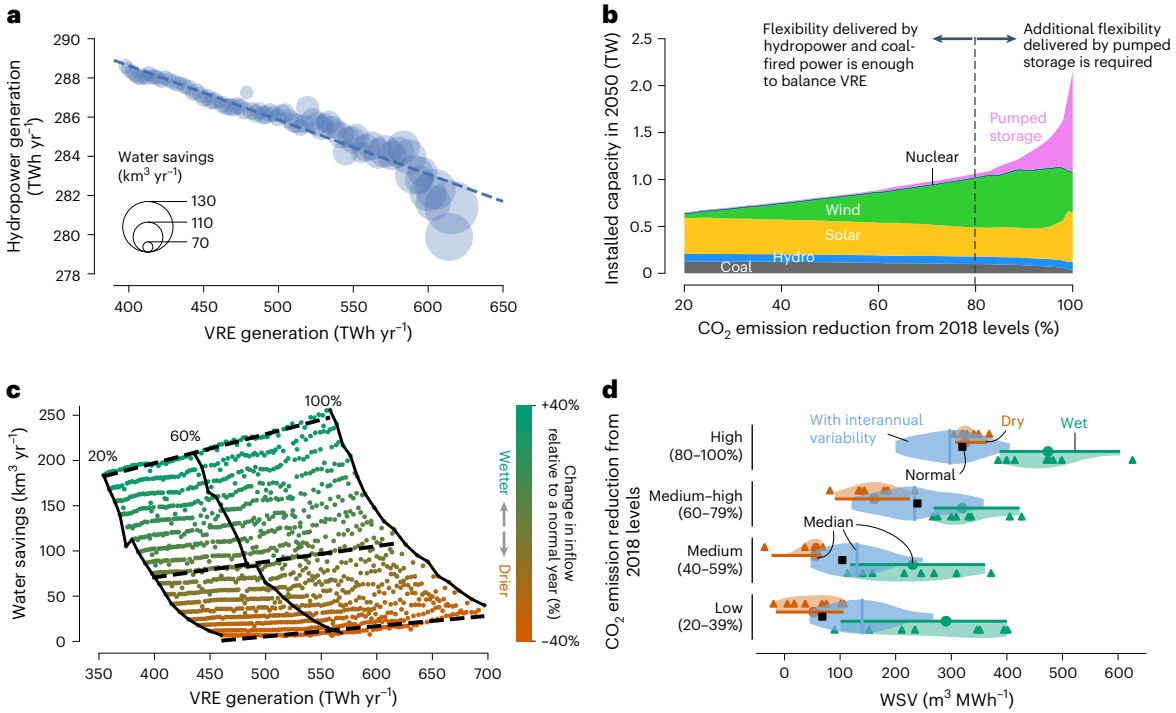

Fig. 3 | Water sustainability value of VRE. a, Annual hydropower production and water savings (scaled by circle size) versus VRE generation across all carbon emission reduction scenarios. The trend line (dashed line) was obtained by ordinary least-squares linear fitting between VRE generation and hydropower generation. **b**, Stacked area plot showing how the planned capacity of different technologies in 2050 varies with the degree of decarbonization. **c**, Variation of water savings with VRE generation and reservoir inflow. Each dot represents a combination of a carbon emission reduction scenario and an inflow scenario. Dots of the same colour represent one inflow scenario across all carbon emission reduction scenarios. The black dashed lines (from top to bottom) are linear fitting lines for scenarios with 40% wetter, normal and 40% drier inflow conditions. The black solid lines represent a certain carbon emission reduction scenario (that is, 20%, 60% and 100%). **d**, Uncertainties in the WSV across a dry inflow (brown line; $n = 8$), a wet inflow (green line; $n = 8$) and an inflow considering interannual variability (light-blue violin-shaped area; $n = 100$) for different ranges of decarbonization. The median values of WSV estimated from dry inflow, wet inflow and inflow with interannual variability are represented by brown dots, green dots and vertical blue lines, respectively. The black squares represent the WSV under normal inflow conditions. The brown and green triangles represent the values of WSV estimated from dry inflow and wet inflow used to derive statistics.

being supplied in the power mix to match demand, directly substituting carbon-emitting electricity. Timing effects refer to more hydropower being generated at the 'right' time (for example, night-time) when VRE generation is low, which can lower the curtailment rate of VRE (Fig. 2c) and thereby indirectly substitute carbon-emitting electricity. Timing effects become more pronounced under AdaptiveHydro operation than under FixedHydro operation (Fig. 4 and Supplementary Fig. 6). This is evidenced by the sub-daily operation process in which AdaptiveHydro tends to shift hydropower generation from daytime to night-time periods when VRE is less available (Fig. 4 and Supplementary Fig. 6), whereas under FixedHydro, hydropower generation (Fig. 4 and black lines in Supplementary Fig. 6) is still largely prioritized during the daytime (to shave peak load). As decarbonization becomes more ambitious, volume effects become stronger (because of a growing penetration of VRE; Fig. 3a,b) and are further reinforced by timing effects (because of enhanced flexibility; Supplementary Fig. 6). Together, they drive a much larger reduction in VRE curtailment (Fig. 2c) as well as total system costs (Fig. 2a). In addition, we found that as VRE integration increases (that is, stronger volume effects), hydropower plants tend to operate at higher water heads in AdaptiveHydro operation (Supplementary Fig. 7). This not only enhances hydropower flexibility, but also reduces the volume of water required to generate an equivalent amount of electricity. As a result, greater water savings can be achieved under AdaptiveHydro.

Intriguingly, we also found an opposite response of water and cost savings to inflow variabilities. The gains in VRE-driven water savings are substantially smaller in dry years than in wet years (Fig. 3d). This is in line with our expectations because reservoir inflow decreases in dry years, leading to declined hydropower production (Supplementary Fig. 8a). As a certain proportion of water still needs to be kept in reservoirs and pass through turbines to generate hydropower and provide flexibility services, less water can be saved for non-hydro purposes. In contrast to water savings, cost savings delivered by flexible hydropower are higher in dry years than in wet years (Fig. 2d). This counterintuitive finding can be explained by the fact that although inflows in dry years reduce hydropower generation (Supplementary Fig. 8a), AdaptiveHydro operation does not require much additional investment in pumped storage hydropower (Supplementary Fig. 9l). This is because of the undiminished timing effects in AdaptiveHydro, in which the joint optimization of flexible hydropower can still maintain relatively high flexibility and continually support volume effects under high VRE penetration (Supplementary Figs. 10 and 11). However, if hydropower is not adaptively operated (FixedHydro), to aid increased VRE integration under drier conditions, investment in storage-driven flexibility (provided by pumped storage hydropower) will need to be linearly scaled up (Supplementary Fig. 9l) to make up for the loss of generation-driven flexibility (provided by reservoir hydropower), substantially increasing total system costs. These findings demonstrate that, in addition to decarbonization policies (Figs. 2b and 3b), inflow variabilities can also drive structural changes in the optimal mix of energy portfolios (Supplementary Fig. 9). A changing climate with more unpredictable inflows could further complicate the trade-offs between long-term investment (considering cost savings) and environmental sustainability concerns (considering water savings).

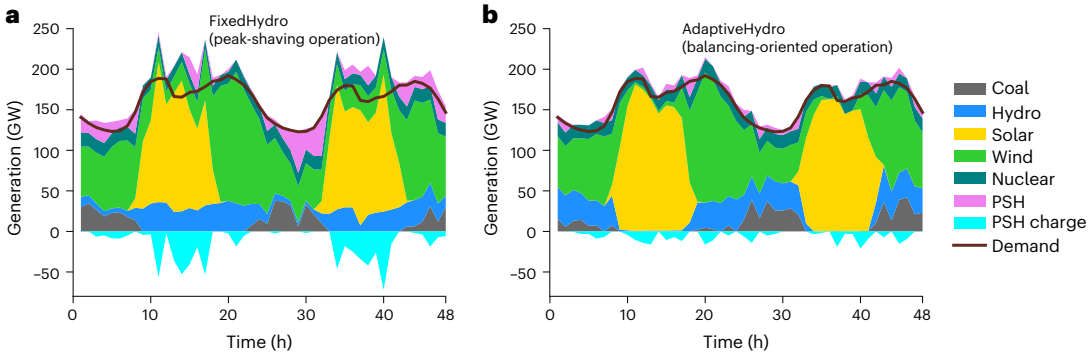

Fig. 4 | Energy generation portfolios and load demand. a,**b**, Hour-by-hour energy generation portfolios and load demand for the CSG during the spring of 2045 for a zero-carbon emission scenario under FixedHydro (**a**) and AdaptiveHydro (**b**) operation schemes. Negative values denote the charging of storage. PSH, pumped storage hydropower.

Our study also suggests that AdaptiveHydro can deliver huge non-monetary benefits that were previously overlooked. Our back-of-the-envelope analysis estimates that an average 57.2 Mt of carbon emissions can be avoided each year in high carbon emission reduction scenarios (see Supplementary Note 4 for methodological details) if hydropower operations are shifted from peak-shaving-oriented operation to balancing-oriented operation. These avoided emissions are equivalent to 10.7% of the total carbon emissions of the electricity sector in the CSG in 2018 (536.9 Mt)[21]. In addition to these carbon abatements, higher VRE penetration simultaneously improves water availability facilitated by large-scale hydropower flexibility and thus leads to additional water savings, especially under deeper decarbonization scenarios. For instance, in a normal inflow year, if the CSG achieves a 100% cut in 2050 carbon emissions from 2018 levels, 123.8 km^3 of water can be preserved each year to support non-hydro purposes (Fig. 3a), for example, managed aquifer recharge[22]. Volumetrically, that is more than twice the annual agricultural water demand (60.2 km^3)[23] of the CSG and over three times the reservoir storage of the Three Gorges Dam (Fig. 1a), the world's largest hydropower dam with a 39.3 km^3 maximum storage capacity[23].

It should be noted that a few factors not considered in our analysis may bias our estimates of cost savings and the WSV. On the one hand, our current analysis of cost savings and the WSV may be conservative because we did not consider small-reservoir and run-of-river hydropower plants or reduced cooling water consumption due to the phasing out of coal-fired power plants[24]. Consideration of these additional water savings could lead to a higher estimate of the WSV. On the other hand, our analysis could potentially overestimate cost savings and the WSV as we did not consider sediment trapping in reservoirs[25], which reduces storage capacity and therefore jeopardizes hydropower flexibility. In addition, reservoir operations in our study were optimized in a deterministic way, assuming perfect inflow forecast without errors. In reality, uncertain and volatile inflow conditions complicate reservoir operations, especially during flood seasons, as power grid dispatchers tend to adopt conservative dispatching strategies for flood control purposes and therefore power generation may be sacrificed. This causes hydropower operation to deviate from the optimal state and thus the anticipated cost savings and WSV are hard to achieve. Improving inflow forecast[26] and reducing sediment trapping in reservoirs[25] are crucial to fully tap the potential of hydro–VRE complementarity to maximize cost savings and the WSV. Additionally, we did not address certain environmental concerns, such as total dissolved gas constraints, which could limit maximum discharge and reduce hydropower flexibility, leading to lower cost savings. Moreover, our model set-up does not consider the dynamic interactions between water savings and changes in the water head. A more complex water management analysis is needed towards a more accurate quantification of water savings. Last but not the least, we did not consider the dynamics of the electricity market, which could potentially lead to an overestimation of the benefits of AdaptiveHydro operations. This is because, in practice, hydropower utilities may lack the necessary incentives to transition from FixedHydro to AdaptiveHydro operations. To encourage such a shift, it is essential to implement suitable cost and revenue allocation strategies, such as the transfer of payments of regional transmission organization to hydropower producers[16].

While our study focused on China's CSG, the PREP-SHOT model developed here can be readily applied to other renewable-rich regions (for example, Southeast Asia, West Africa and the Amazon) to scale up VRE and guide low-impact hydropower development[27,28]. This is facilitated by the recent proliferation of publicly available data related to climate (for example, reanalysis[29]), hydrology (for example, natural inflow[30] and reservoir and hydropower characteristics) and socioeconomics (for example, technology cost parameters[31] and capacity factors of VRE[32]). For data that are not readily available, such as national or sub-national hourly electricity demand, existing well-established methods[33] can be used to generate proxy data and use them in sensitivity analyses to deliver robust findings. However, big challenges may exist, especially across regions with transboundary rivers, where the joint optimization of cascade reservoirs across countries requires improved cross-border cooperation.

Methods

Energy expansion optimization model

Model overview. We have developed a transparent, modular and open-source energy expansion model, PREP-SHOT (see Supplementary Fig. 1 for a high-level structural overview), to investigate how short-term cascade hydropower reservoir operation affects long-term energy planning. Compared with existing energy planning models, which treat hydropower as fixed processes[17], overlook the dynamic nature of water heads[16] or simply aggregate multiple hydropower stations into a single unit[14], a unique feature of PREP-SHOT is that it explicitly considers the plant-level water head dynamics (that is, time-varying water head and storage) and system-level network topology of all hydropower stations within a regional grid. This allows us to better capture the multi-scale dynamic feedbacks between hydropower operation and energy system expansion, as well as to realistically simulate the magnitude and spatiotemporal variability of hydropower output, especially in regions with a large number of cascade hydropower stations. PREP-SHOT uses a multi-scale, constrained optimization approach that jointly considers both short-term (for example, hourly to daily) dispatch processes and long-term (for example, annual to decennary) capacity expansion decisions in different planning zones and horizons. The goal of PREP-SHOT is to identify optimal expansion pathways of power system decisions (for example, technology portfolio, transmission

capacity and generation process) that minimize the total system cost (that is, variable and fixed O&M cost, fuel cost and investment cost) subject to a set of power balance, water balance and available resources constraints. Mathematically, the objective function of PREP-SHOT is formulated in Supplementary Equation (1), subject to the following 10 sets of constraints:

1. Lifetime constraints (Supplementary Equations (11) and (12) in Supplementary Note 3, similarly hereafter)
2. Carbon emission constraints (Supplementary Equations (13) and (14))
3. Power balance constraints (Supplementary Equation (15))
4. Transmission constraints (Supplementary Equations (16)–(18))
5. Power output constraints (Supplementary Equations (19)–(23))
6. Power output variation constraints (Supplementary Equations (24)–(26))
7. Energy storage constraints (Supplementary Equations (27)–(32))
8. Water balance constraints (Supplementary Equations (33)–(35))
9. Reservoir outflow constraints (Supplementary Equations (36)–(38))
10. Reservoir storage constraints (Supplementary Equations (39)–(41))

Cost estimations and model constraints are detailed in Supplementary Notes 2 and 3. We implemented two methods (that is, the simplex method and the barrier method) to solve the above linear programming problem. Solutions were selected from the method that obtained the optimal conditions with less computational time.

Representation of short-term cascade reservoir operations. The power output of hydropower station s at hour h of month m of year y ($\text{power}^{\text{hydro}}_{s,h,m,y}$) was determined by the net water head ($\text{head}^{\text{net}}_{s,h,m,y}$) and the discharge flowing through the turbines (called generation flow, $\text{outflow}^{\text{gen}}_{s,h,m,y}$) according to the following equation:

$$\text{power}^{\text{hydro}}_{s,h,m,y} = \eta_s \times \rho \times g \times \text{outflow}^{\text{gen}}_{s,h,m,y} \times \text{head}^{\text{net}}_{s,h,m,y} \quad (1)$$

where η_s is the output efficiency of the hydropower station s, ρ is the density of water (1,000 kg m^{-3}) and g is the acceleration of gravity (9.8 m s^{-2}). The output efficiency η_s is constant for a specific hydropower station. Here, we treated $\text{outflow}^{\text{gen}}_{s,h,m,y}$ as a decision variable and calculated $\text{head}^{\text{net}}_{s,h,m,y}$ using a set of non-linear equality constraints. Specifically, $\text{head}^{\text{net}}_{s,h,m,y}$ can be calculated by subtracting the tailrace water level ($z^{\text{tailrace}}_{s,h,m,y}$) and total water head loss ($\text{head}^{\text{loss}}_{s,h,m,y}$) from the average forebay water level $\left((z^{\text{forebay}}_{s,h-1,m,y} + z^{\text{forebay}}_{s,h,m,y})/2\right)$ between hour $h-1$ and h as follows (see Supplementary Fig. 12 for a detailed illustration):

$$\text{head}^{\text{net}}_{s,h,m,y} = \frac{z^{\text{forebay}}_{s,h-1,m,y} + z^{\text{forebay}}_{s,h,m,y}}{2} - z^{\text{tailrace}}_{s,h,m,y} - \text{head}^{\text{loss}}_{s,h,m,y} \quad \forall s,h,m,y \quad (2)$$

$z^{\text{tailrace}}_{s,h,m,y}$ can be determined from the tailwater rating curve (Supplementary Fig. 13a) through a piecewise linear function ($f^{\text{zq}}_s(\cdot)$) that empirically links $z^{\text{tailrace}}_{s,h,m,y}$ with the total released flow (that is, the sum of the generation flow ($\text{outflow}^{\text{gen}}_{s,h,m,y}$) and the released flow over spillways ($\text{outflow}^{\text{spillage}}_{s,h,m,y}$)):

$$z^{\text{tailrace}}_{s,h,m,y} = f^{\text{zq}}_s\left(\text{outflow}^{\text{spillage}}_{s,h,m,y} + \text{outflow}^{\text{gen}}_{s,h,m,y}\right) \quad \forall s,h,m,y \quad (3)$$

$\text{head}^{\text{loss}}_{s,h,m,y}$ is determined by a quadratic function of $\text{outflow}^{\text{gen}}_{s,h,m,y}$ following the method suggested in ref. 34:

$$\text{head}^{\text{loss}}_{s,h,m,y} = K_s \times \left(\text{outflow}^{\text{gen}}_{s,h,m,y}\right)^2 \quad \forall s,h,m,y \quad (4)$$

where K_s is a constant representing the experimental water head loss coefficient.

Similarly, forebay water level ($z^{\text{forebay}}_{s,h,m,y}$) is a function of reservoir storage ($\text{storage}^{\text{reservoir}}_{s,h,m,y}$) and thus can be determined by the stage-storage curve (Supplementary Fig. 13b) as follows:

$$z^{\text{forebay}}_{s,h,m,y} = f^{\text{zs}}_s\left(\text{storage}^{\text{reservoir}}_{s,h,m,y}\right) \quad \forall s,h,m,y \quad (5)$$

where $f^{\text{zs}}_s(\cdot)$ represents the piecewise linear function of the stage-storage curve. While it is computationally challenging to estimate water head dynamics due to the discrete, non-convex, non-linear and high-dimensional nature of the optimization problem[35], to balance the trade-off between numerical accuracy and computational efficiency, PREP-SHOT implements a simulation-based iterative procedure[36] to explicitly calculate the time-varying net water heads instead of using traditional piecewise linear functions[35] or fitted non-linear functions[37]. The simulation-based iterative procedure involves the following five steps (see Supplementary Fig. 14 for the complete flow chart):

1. Set the initial net water head ($\text{head}^{\text{net}}_{s,h,m,y}$, here the designed water head of a hydropower station is used as the initial net water head) for hydropower station s at hour h of month m of year y and the number of iterations $n = 1$.
2. Solve the PREP-SHOT model using the initial (or previously updated) net water head. Because a fixed net water head is set, the original non-linear optimization problem can be simplified to a linear programming model that can readily be solved.
3. Obtain $\text{outflow}^{\text{spillage}}_{s,h,m,y}$, $\text{outflow}^{\text{gen}}_{s,h,m,y}$ and $\text{storage}^{\text{reservoir}}_{s,h,m,y}$ from the optimal solutions obtained in Step 2 and then substitute them into equations (2)–(5) to compute the intermediate water head ($\text{head}^{\text{intermediate}}_{s,h,m,y}$).
4. Calculate the relative error (RE) between $\text{head}^{\text{intermediate}}_{s,h,m,y}$ and $\text{head}^{\text{net}}_{s,h,m,y}$ as follows:

$$\text{RE} = \frac{1}{|\mathcal{S}|\times|\mathcal{H}|\times|\mathcal{M}|\times|\mathcal{Y}|} \times \sum_{s\in\mathcal{S}}\sum_{h\in\mathcal{H}}\sum_{m\in\mathcal{M}}\sum_{y\in\mathcal{Y}} \frac{\text{abs}\left(\text{head}^{\text{intermediate}}_{s,h,m,y} - \text{head}^{\text{net}}_{s,h,m,y}\right)}{\text{head}^{\text{net}}_{s,h,m,y}} \quad (6)$$

where abs(·) is a function that returns the absolute value of a number and |·| represents the number of elements in the set (see Supplementary Note 1 for detailed description of all sets).

5. Compare the RE with a given threshold ϵ and n with a predefined maximum number of iterations N. If RE ≤ ϵ or $n \geq N$, stop the iteration and obtain the optimal solutions from Step 2. Otherwise, update $\text{head}^{\text{net}}_{s,h,m,y}$ according to the following formula, update $n := n + 1$ and then return to Step 2:

$$\text{head}^{\text{net}}_{s,h,m,y} := \text{head}^{\text{net}}_{s,h,m,y} + \alpha \times \left(\text{head}^{\text{intermediate}}_{s,h,m,y} - \text{head}^{\text{net}}_{s,h,m,y}\right) \quad (7)$$

where α represents the step size (varying from 0 to 1) used to update the net water head during the iteration. It is a parameter that controls the convergence speed of the numerical algorithm. Here, we set $\alpha = 1/n$ to balance the solving speed and accuracy.

The default setting of the PREP-SHOT model described above is referred to as AdaptiveHydro, in which hydropower operations can be adjusted flexibly up to a certain extent (rather than using a separately optimized fixed operation process) to balance load demand with anticipated future increases in VRE penetration. This is similar to the balancing-oriented operation detailed in ref. 2. To quantify the benefit of short-term flexible hydropower operation for the long-term energy expansion, we also designed a baseline FixedHydro scenario, in which we directly solved an energy expansion model with a predefined hydropower output process (that is, constant input with a fixed reservoir operation process) rather than treating hydropower output processes as decision variables (that is, dynamic input with an

adaptive reservoir operation process that can be optimized). Here, the fixed hydropower output process was obtained by maximizing the benefit of peak-shaving and hydroelectricity generation, a typical strategy towards peak-shaving-oriented operation[8]. In contrast to AdaptiveHydro, which tries to minimize total system-wide cost (Supplementary Equation (1)), optimization in FixedHydro tries to minimize the sum of squared remaining demand (F; equation (8)), which has the following form:

$$\min F = \sum_{z\in\mathcal{Z}} \sum_{m\in\mathcal{M}} \sum_{h\in\mathcal{H}} \left(\text{demand}_{h,m,z} - \sum_{s\in\mathcal{S}_z} \text{power}^{\text{hydro}}_{h,m,s} \right)^2 \quad (8)$$

where $\text{demand}_{h,m,z}$ is the total electric demand at hour h of month m in zone z and $\text{power}^{\text{hydro}}_{h,m,s}$ is the power output of hydropower station s at hour h of month m. Here, the optimization in FixedHydro shares the same sets of constraints (that is, power output, power output variation, water balance, reservoir outflow and reservoir storage) as AdaptiveHydro. Similarly, the simulation-based iterative procedure described above was also used here to estimate the net water heads in a computationally efficient manner.

Model configuration. PREP-SHOT was designed as a multi-technology, multi-node and intertemporal optimization model. PREP-SHOT supports multi-technology expansion and groups all energy technologies into four categories: 'hydro', 'storage', 'non-dispatchable' and 'dispatchable' technologies. As we were particularly interested in the value of flexible hydropower, PREP-SHOT considers a location-specific, plant-level 'hydro' generation process, rather than aggregating all hydropower generation at a larger spatial scale (province level in this study), a typical strategy widely adopted in other existing models[14]. 'Storage' technologies in PREP-SHOT typically include pumped storage hydropower and lithium-ion batteries. We assumed that these technologies can discharge when the total power output of all technologies cannot meet the total electric demand and the amount of discharged electricity is limited only by the stored electricity level. Excess electricity will be charged if the total power output of all technologies exceeds the total electric demand. In real-world applications, it is typically avoided to have 'storage' technologies charged and discharged simultaneously[38]. This practice stems from the goal of minimizing system costs, aiming to prevent any unnecessary loss of electricity. While our model does not enforce a specific constraint regarding this, the principle of cost minimization inherent in our model ensures that this practice is upheld. 'Non-dispatchable' technologies refer to VRE that can be curtailed when total supply exceeds total demand, mostly solar PV and wind power. Such technologies are limited by capacity factors driven by instantaneous weather conditions that are location-dependent (see Supplementary Note 5 for details). In contrast to the 'non-dispatchable' technologies, 'dispatchable' technologies can be controlled within a certain range and usually serve as complementary and flexible power supply. These include coal-fired plants, nuclear plants and gas plants, among others, and can be dispatched flexibly between technical minimum output and installed capacity (see Supplementary Note 3 for details).

PREP-SHOT also includes a zone index z for decision variables and parameters that are zone-specific. This feature allows energy planners to model large-scale interconnected regional grids with multiple spatial nodes (for example, provinces and countries), where electricity can be transmitted between different nodes through existing or planned transmission lines. PREP-SHOT applies a transportation model (also called pipeline model) to simulate the power transmission between spatial nodes. This model assumes that the transmitted power is limited by only the capacity of the transmission lines between two spatial nodes[39]. In addition, all transmission lines are bidirectional, but simultaneous bidirectional transmission is physically not allowed. Similar to the 'storage' technologies, simultaneous bidirectional transmission is automatically prohibited to align with the objective of minimizing system costs. In this study, the geometric centre of each province in the CSG was selected as the location of the node to calculate the distance between province pairs. This distance was then used to calculate the cost of newly built transmission lines (Supplementary Table 3).

On top of the multi-node feature, PREP-SHOT also introduces a time domain with a multi-layer time slice (h,m,y) to support intertemporal optimization. For instance, multi-period near-future and long-term investment decisions can be optimized over the entire planning horizon. Intertemporal constraints on short-term power output processes (for example, power output variation constraints) can also be explicitly represented (see Supplementary Note 2 for detailed cost estimations and Supplementary Note 3 for the power output variation constraints used for the intertemporal optimization). To maintain computational tractability while also realistically representing both long-term investment decisions and short-term operational details of the energy system, PREP-SHOT implements a three-level time slice to solve the intertemporal optimization. The top-level time slice is Year (y), characterizing the investment period at the annual timescale. As it is computationally expensive to optimize the high-dimensional energy system for a full year (8,760 h) over the entire planning horizon (usually a few decades), PREP-SHOT introduces a second-level time slice, Month (m), to reduce the computational burden, while at the same time still representing seasonal variability, which is especially relevant for hydropower. The third-level time slice is Hour (h), at which scale PREP-SHOT can realistically model the short-term (for example, hourly) variability of energy demand, the intermittency of VRE and the operational flexibility of hydropower.

In this study, we ran PREP-SHOT over 48 consecutive hours for two representative days in each season (that is, January–March, April–June, July–September and October–December) for seven modelled years (2018, 2025, 2030, 2035, 2040, 2045 and 2050). There are five spatial nodes in PREP-SHOT, representing the five provinces (Guangdong, Guangxi, Guizhou, Hainan and Yunnan; see Fig. 1a) in the CSG. PREP-SHOT was built using Python 3.8.14 (https://www.python.org) with Pyomo 5.7.3 (https://github.com/Pyomo/pyomo) and solved by Gurobi 9.5.0 (https://www.gurobi.com/).

Experimental design and scenarios

Carbon emission reduction scenarios. In this study, we considered 81 carbon emission reduction scenarios (Fig. 1c) to examine to what extent the value of hydropower flexibility varies with the decarbonization level. These scenarios were designed on the basis of China's recent pledge to peak carbon dioxide emissions by 2030 and to achieve carbon neutrality by 2060. We assumed that the percentage carbon emission reduction in the period 2018–2050 varies from 20% (less decarbonized) to 100% (fully decarbonized) with a discrete step size of 1% (that is, 20%, 21%, …, 99%, 100%). For each scenario, we assumed a same upper bound of annual carbon emissions over the period 2018–2030, which was set to the CO_2 emissions from power generation in the CSG in 2018 (that is, 536.9 Mt)[21]. From 2030 to 2050, we assumed a linear decrease in the upper bound of CO_2 emissions in each scenario.

Inflow scenarios. We designed 117 inflow scenarios (1 normal, 8 wet, 8 dry and 100 interannual variability) to investigate how inflow variability affects our results. We used the estimated inflow in 2018 (see details in the Natural inflow data section below) to represent normal conditions as the baseline scenario. To obtain the ith inflow scenario ($\text{inflow}^{\text{net}}_{s,h,m,y,i}$) reflecting drier- or wetter-than-normal conditions, we included a constant factor (ω_i) to scale the baseline scenario ($\text{inflow}^{\text{net}}_{s,h,m,y}$) as follows:

$$\text{inflow}^{\text{net}}_{s,h,m,y,i} = \text{inflow}^{\text{net}}_{s,h,m,y} + \omega_i \times \text{abs}\left(\text{inflow}^{\text{net}}_{s,h,m,y}\right) \quad (9)$$

where ω_i ranges from −40% to 40% in increments of 5% excluding 0% (−40%, −35%, ⋯, −5%, 5%, ⋯, 35%, 40%). We applied the estimated net inflow in 2018 to future representative years (2025, 2030, 2035, 2040, 2045 and 2050) for these 17 inflow scenarios. Given that we only had streamflow records for one year (that is, 2018), which cannot capture the year-to-year inflow variability, we used the Global Reach-scale A priori Discharge Estimates for SWOT (GRADES) dataset[30], a 40-year (1979–2018) global streamflow reanalysis. To factor in the uncertainty of inflow interannual variability, we used Bootstrap to randomly sample seven representative years from the 40-year pool of historical bias-corrected GRADES and repeated this process 100 times. We used a simultaneous sampling approach to obtain historical streamflow data from the same time period for all hydropower plants. This allowed us to maintain the spatial correlation between different hydropower plants, which is important to accurately capture realistic hydraulic connections for watersheds with cascade reservoirs.

Key data assumptions

Technology and cost assumptions. In this study, we considered six primary technologies, that is, 'dispatchable' coal-fired and nuclear power, 'non-dispatchable' solar and onshore wind power, conventional hydropower and pumped storage hydropower. We took 2018 (the most recent year with available data) as the starting year to define the initial installed capacity of each technology (Supplementary Table 4), derived from various sources, including the *China Power Statistics Yearbook 2021*[40], the National Energy Administration[41] and China Nuclear Energy Association[42]. Cost parameters are summarized in Supplementary Table 5. Projected cost reductions (percentage changes) between 2018 and 2050 were derived from the National Renewable Energy Laboratory's annual technology baseline assessment in 2020[31]. The investment cost of conventional hydropower and pumped storage hydropower was assumed to be constant over the entire planning horizon. Changes in investment cost for other technologies (that is, wind, solar, coal-fired and nuclear power) are shown in Supplementary Fig. 15. The investment cost of ultrahigh vacuum direct current transmission lines was set to ¥900 MW^{-1} km^{-1} (where ¥ is Chinese yuan; ref. 21). The province-level capacity of transmission lines was taken from ref. 5 (Supplementary Table 6). We assumed an average 94% efficiency of all transmission lines based on the province-level line loss rate documented in China's 2021 power industry development report[21].

The projected carbon content (that is, CO_2 emissions per unit of generated coal-fired electricity) in each modelled year was estimated by extrapolating historical (2005–2020)[40] trends using the optimal piecewise linear fitting approach[43] (Supplementary Fig. 16). Three predefined line segments were used and breakpoints were determined by minimizing the total sum of squared errors between fitted values and actual values. We also factored in the age-capacity relationship of existing power stations in each province when we estimated the existing capacity of technologies (see Supplementary Table 7 for the age and corresponding capacity of coal-fired power plants in 2018 obtained from the Global Energy Monitor's Global Coal Plant Tracker[44]).

Demand profile. Province-level hourly electric demand in 2018 was compiled by the CSG[45]. The near-future (2018–2030) growth rate of demand was obtained from ref. 46. We assumed a 40% (for 2030–2040) and 67% (for 2040–2050)[39,47] decrease in the growth rate relative to 2018–2030 (Supplementary Table 8). To estimate the required load demand for each representative year in the future, we scaled the observed load demand in 2018 using the projected annual average growth rate from 2018 to 2050[47]. As it is computationally extremely expensive to run PREP-SHOT at the hourly time step for the entire year, we focused on a representative 2-day period in spring (January–March), summer (April–June), autumn (July–September) and winter (October–December). Such seasonal-dependent representative load demand profiles were generated on the basis of a *k*-nearest neighbours algorithm[48], which can identify the optimal non-linear alignment between two time series via dynamic time warping. We first obtained the optimal clustered demand profiles for two consecutive days (48 h in total, from 00:00 to 23:00). We then searched within each season to find the representative date whose actual 48-h consecutive load demand best matches the clustered load demand time series by minimizing the Euclidean distance between these two time series (Supplementary Fig. 17). The obtained representative dates in each season were 10–11 March in spring, 8–9 June in summer, 17–18 August in autumn and 27–28 November in winter (see Supplementary Fig. 18 for the seasonal representative load demand profiles for each province in the CSG) and remained consistent across all scenarios, including normal, dry, wet and interannual variability flows. It should be noted that the selection of representative periods in this study was focused solely on electricity and, therefore, may not accurately represent water use patterns. Future research should incorporate changes in both electricity and water to identify more suitable representative periods.

Natural inflow data. Forty-six hydropower stations with an installed capacity of over 300 MW were selected for the analysis, according to data availability. The cascade topology of these selected hydropower stations is shown in Supplementary Fig. 2 and their key characteristics are summarized in Supplementary Table 1. As the natural inflow of each reservoir cannot be observed directly (only the outflow downstream of each reservoir is measured), we used net inflow instead. Here, net inflow factors in the net effect of evaporation, upstream withdrawal and precipitation on the control area of the reservoir. The net inflow can be derived using the water balance principle as follows (Supplementary Fig. 19):

$$\begin{aligned}\text{inflow}^{\text{net}}_{s,h,m,y} = {} & \frac{\text{storage}^{\text{reservoir}}_{s,h,m,y}}{\Delta h} + \text{outflow}^{\text{total}}_{s,h,m,y} \\ & - \frac{\text{storage}^{\text{reservoir}}_{s,h-1,m,y}}{\Delta h} \\ & - \sum_{\text{su}\in\mathcal{IU}_s}\left(\text{outflow}^{\text{total}}_{\text{su},h-\tau_{\text{su},s},m,y}\right) \quad \forall s,h,m,y\end{aligned} \tag{10}$$

where $\text{inflow}^{\text{net}}_{s,h,m,y}$ is the net inflow into hydropower station s at hour h in month m of year y, $\text{storage}^{\text{reservoir}}_{s,h,m,y}$ represents the observed storage of hydropower station s at hour h in month m of year y, Δh represents the simulation time step (that is, 1 h), $\text{outflow}^{\text{total}}_{s,h,m,y}$ refers to the observed total outflow, which is the sum of the spillage outflow ($\text{outflow}^{\text{spillage}}_{s,h,m,y}$) and generation outflow ($\text{outflow}^{\text{gen}}_{s,h,m,y}$), $\mathcal{IU}_s$ represents the set of all immediate upstream hydropower stations of hydropower station s, $\tau_{\text{su},s}$ is a constant representing water travel time between hydropower station s and its immediate upstream hydropower station su. It should be noted that some negative values of estimated net inflow, likely caused by evaporation and water withdrawal to meet other needs (for example, agricultural irrigation), were retained in our calculations.

Capacity factors of solar and wind energy. Capacity factors (CFs) of VRE were derived using the Modern-Era Retrospective analysis for Research and Application version 2 (MERRA-2) reanalysis product[49]. Seasonal-varying province-averaged CF over the representative days were estimated according to the following three steps:

1. Calculate the pixel-level (0.625° × 0.5° spatial resolution) CF using the surface incoming shortwave radiation, the top-of-the-atmosphere incoming shortwave radiation and the temperature at 2 m (for solar power) and wind speed at 10 and 50 m (for wind power; see Supplementary Note 5 for details).
2. Calculate the province-level CF by spatially averaging all grid cells in each province weighted by the pixel area.

3. Scale the province-level CF at hour h of month m by the ratio of the average CF in 2018 (CF_{2018}) and the long-term historical (1980–2019) averaged CF (CF_{hist}) as follows:

$$CF^{scaled}_{h,m,2018} = CF_{h,m,2018} \times \frac{CF_{2018}}{CF_{hist}} \quad (11)$$

Then we selected the scaled CF ($CF^{scaled}_{h,m,2018}$) for the representative dates (Supplementary Fig. 4). Here, we applied $CF^{scaled}_{h,m,2018}$ to each representative year by assuming unchanged climatology drivers for solar and wind CFs.

Benefits of hydropower flexibility

WSV of VRE. The WSV ($m^3\,yr^{-1}\,MWh^{-1}$) of VRE measures how much water can be conserved for non-hydropower purposes each year per megawatt hour increase in electricity generated by VRE, specifically from solar and wind energy. To estimate WSV, we introduced a new term, μ (¥ m^{-3}), which characterizes the marginal value of each unit of water saved, into the objective function, acknowledging the fact that the water saved for other beneficial uses (for example, irrigation) can compensate part of the total system costs. As it is not possible to obtain a reliable estimate of μ, we used the price of irrigation water as a proxy of μ given the fact that the use of water for irrigation dominates our study area. We found that the total water savings over the entire planning horizon are not sensitive to the choice of μ (Supplementary Fig. 20), whose range was adjusted according to ref. 50 and the final value was determined through a trial-and-error process. Empirically, WSV can be estimated from the linear slope fitted between water savings (aggregated across all reservoirs) and total VRE generation (Supplementary Fig. 21a). Here, we used a piecewise linear fit instead of fitting all data points using a single linear function because of the inherent non-linear relationship between water savings and total VRE generation. To obtain a robust fit (which requires sufficient data samples) while also capturing the non-linearities (which requires sufficient segments), the piecewise line fit was performed over four groups according to the degree of decarbonization: low (20–39%), medium (40–59%), medium–high (60–79%) and high (80–100%). Within each group, we pooled all data points to obtain the optimal slope and estimate the 95% confidence interval using Bootstrap (10,000 times).

Curtailment rate of renewables. The curtailment rate (CR) of VRE is defined as the ratio between curtailed renewable generation and total potential generation:

$$CR = \frac{\sum_{z\in\mathcal{Z}}\sum_{y\in\mathcal{Y}}\sum_{m\in\mathcal{M}}\sum_{h\in\mathcal{H}}\sum_{e\in\mathcal{E}} gen_{h,m,y,z,e}}{\sum_{z\in\mathcal{Z}}\sum_{y\in\mathcal{Y}}\sum_{m\in\mathcal{M}}\sum_{h\in\mathcal{H}}\sum_{e\in\mathcal{E}}\left(cap^{existing}_{y,z,e} \times CF_{h,m,y,z,e}\right)} \quad (12)$$

where $gen_{h,m,y,z,e}$ represents the generation of non-dispatchable technology e for zone z at hour h in month m of year y, $CF_{h,m,y,z,e}$ is the CF of non-dispatchable technology e at hour h in month m of year y and $cap^{existing}_{y,z,e}$ represents the existing installed capacity of non-dispatchable technology e in zone z in year y.

Model limitations

It is important to note that our framework relies on simplified modelling assumptions to balance the trade-offs between model representability and computational efficiency. For example, in actual hydropower operations, shifting from FixedHydro to AdaptiveHydro can lead to increased operating costs due to more frequent ramping and start/stop of hydropower plants. While directly including such constraints in PREP-SHOT would more accurately quantify system-level costs and water savings, it would also require optimizing ~183,000 additional binary variables, making the optimization problem intractable, particularly for sensitivity analyses with a large number of scenarios. Despite these limitations, our post analysis shows that the attained cost savings are only slightly reduced by 3.69–6.36% (Supplementary Fig. 22) with almost no impact on water savings (reduced by 0.09–0.32%; Supplementary Fig. 23) if the start/stop constraints are considered. Another important consideration is the representation of complex river dynamics. The default setting of PREP-SHOT uses a constant travel time in river routing processes as this allows us to substantially reduce the computational burden associated with the complex hydraulic connections of cascade reservoirs. Although a more sophisticated river routing method, such as an impulse response function[8], could better capture river dynamics, it would increase the computational burden by more than a factor of five, even for a single experiment. Nevertheless, we found that using a more complex river routing method, such as the impulse response function, does not affect our main conclusions, as the attained cost and water savings remain largely the same (Supplementary Fig. 24).

Reporting summary

Further information on research design is available in the Nature Portfolio Reporting Summary linked to this article.

Data availability

MERRA-2 data can be downloaded from https://disc.gsfc.nasa.gov/datasets?project=MERRA-2. GRADES data can be downloaded from https://www.reachhydro.org/home/records/grades. The river lines and basin boundaries used for map illustration can be downloaded from https://www.hydrosheds.org/products. Dam and reservoir characteristics can be downloaded from https://www.globaldamwatch.org/. All other data used in the optimization are provided in the Supplementary Information and are cited from publicly available sources. Source data are provided with this paper.

Code availability

The energy expansion model PREP-SHOT is available under the GNU General Public License version 3 (GPLv3) and can be downloaded from the GitHub repository (https://github.com/PREP-NexT/PREP-SHOT) of the Pathways for REsilient Planning of water-energy-food Nexus Transformation (PREP-NexT) Lab. The Python scripts used to produce the results in this paper are available upon request from Z.L.

References

1. Dhakal, S. et al. 2022: Emissions Trends and Drivers. In IPCC, 2022: Climate Change 2022: Mitigation of Climate Change (eds Shukla, P. R. et al.) 215–294 (IPCC, Cambridge Univ. Press, 2022).
2. Sterl, S. et al. Smart renewable electricity portfolios in West Africa. *Nat. Sustain.* **3**, 710–719 (2020).
3. Schmitt, R. J. P., Kittner, N., Kondolf, G. M. & Kammen, D. M. Deploy diverse renewables to save tropical rivers. *Nature* **569**, 330–332 (2019).
4. Rich, E. et al. *Hydropower Status Report 2021: Sector Trends and Insights* (International Hydropower Association, 2021).
5. Zhang, J., Cheng, C., Yu, S., Wu, H. & Gao, M. Sharing hydropower flexibility in interconnected power systems: a case study for the China Southern Power Grid. *Appl. Energy* **288**, 116645 (2021).
6. Abdelilah, Y. et al. *Hydropower Special Market Report: Analysis and Forecast to 2030* (International Energy Agency, 2021).
7. Voisin, N., Tidwell, V., Kintner-Meyer, M. & Boltz, F. Planning for sustained water–electricity resilience over the US: persistence of current water–electricity operations and long-term transformative plans. *Water Secur.* **7**, 100035 (2019).
8. Liao, S. et al. Daily peak shaving operation of cascade hydropower stations with sensitive hydraulic connections considering water delay time. *Renew. Energy* **169**, 970–981 (2021).
9. Sterl, S., Fadly, D., Liersch, S., Koch, H. & Thiery, W. Linking solar and wind power in eastern Africa with operation of the Grand Ethiopian Renaissance Dam. *Nat. Energy* **6**, 407–418 (2021).

10. Abdin, I., Fang, Y.-P. & Zio, E. A modeling and optimization framework for power systems design with operational flexibility and resilience against extreme heat waves and drought events. *Renew. Sustain. Energy Rev.* **112**, 706–719 (2019).
11. He, X., Wada, Y., Wanders, N. & Sheffield, J. Intensification of hydrological drought in California by human water management. *Geophys. Res. Lett.* **44**, 1777–1785 (2017).
12. He, X. et al. Solar and wind energy enhances drought resilience and groundwater sustainability. *Nat. Commun.* **10**, 4893 (2019).
13. Turner, S. W., Steyaert, J. C., Condon, L. & Voisin, N. Water storage and release policies for all large reservoirs of conterminous United States. *J. Hydrol.* **603**, 126843 (2021).
14. Dimanchev, E. G., Hodge, J. L. & Parsons, J. E. The role of hydropower reservoirs in deep decarbonization policy. *Energy Policy* **155**, 112369 (2021).
15. Ibanez, E. et al. Enhancing hydropower modeling in variable generation integration studies. *Energy* **74**, 518–528 (2014).
16. Rodríguez-Sarasty, J. A., Debia, S. & Pineau, P.-O. Deep decarbonization in Northeastern North America: the value of electricity market integration and hydropower. *Energy Policy* **152**, 112210 (2021).
17. Siala, K., Chowdhury, A. K., Dang, T. D. & Galelli, S. Solar energy and regional coordination as a feasible alternative to large hydropower in Southeast Asia. *Nat. Commun.* **12**, 4159 (2021).
18. Oikonomou, K., Tarroja, B., Kern, J. & Voisin, N. Core process representation in power system operational models: gaps, challenges, and opportunities for multisector dynamics research. *Energy* **238**, 122049 (2022).
19. *China Southern Power Grid Corporation's Action Plan for Building a New Power System (2021–2030) White Paper* (China Southern Power Grid, 2021).
20. Bakos, G. C. Feasibility study of a hybrid wind/hydro power system for low-cost electricity production. *Appl. Energy* **72**, 599–608 (2002).
21. Pan, L. et al. *Annual Development Report of China's Power Industry 2021* (China Electricity Council, 2021).
22. He, X. et al. Climate-informed hydrologic modeling and policy typology to guide managed aquifer recharge. *Sci. Adv.* **7**, eabe6025 (2021).
23. *China Water Resources Bulletin 2021* (Ministry of Water Resources of the People's Republic of China, 2021).
24. Cheng, Y., Voisin, N., Yearsley, J. R. & Nijssen, B. Thermal extremes in regulated river systems under climate change: an application to the southeastern US rivers. *Environ. Res. Lett.* **15**, 094012 (2020).
25. Xu, B. & He, X. A physics-informed Bayesian storyline approach to assess sediment transport in the Mekong. *Water Resour. Res.* **58**, e2022WR032681 (2022).
26. Liao, S. et al. Multistep-ahead daily inflow forecasting using the ERA-Interim reanalysis data set based on gradient-boosting regression trees. *Hydrol. Earth Syst. Sci.* **24**, 2343–2363 (2020).
27. Schmitt, R. J. P., Bizzi, S., Castelletti, A., Opperman, J. J. & Kondolf, G. M. Planning dam portfolios for low sediment trapping shows limits for sustainable hydropower in the Mekong. *Sci. Adv.* **5**, eaaw2175 (2019).
28. Pokhrel, Y. & Tiwari, A. D. Re-operating dams in the Mekong. *Nat. Sustain.* **5**, 1005–1006 (2022).
29. Hersbach, H. et al. The ERA5 global reanalysis. *Q. J. R. Meteorol. Soc.* **146**, 1999–2049 (2020).
30. Lin, P. et al. Global reconstruction of naturalized river flows at 2.94 million reaches. *Water Resour. Res.* **55**, 6499–6516 (2019).
31. Akar, S. et al. *2020 Annual Technology Baseline* (NREL, 2020); https://atb-archive.nrel.gov/electricity/2020/data.php
32. Pfenninger, S. & Staffell, I. Long-term patterns of European PV output using 30 years of validated hourly reanalysis and satellite data. *Energy* **114**, 1251–1265 (2016).
33. Brinkerink, M., Gallachóir, B. Ó. & Deane, P. Building and calibrating a country-level detailed global electricity model based on public data. *Energy Strategy Rev.* **33**, 100592 (2021).
34. Kishor, N. & Fraile-Ardanuy, J. (eds.) *Modeling and Dynamic Behaviour of Hydropower Plants* (The Institution of Engineering and Technology, 2017).
35. Cheng, C., Wang, J. & Wu, X. Hydro unit commitment with a head-sensitive reservoir and multiple vibration zones using MILP. *IEEE Trans. Power Syst.* **31**, 4842–4852 (2016).
36. Liao, S. et al. Short-term hydro scheduling considering multiple units sharing a common tunnel and crossing vibration zones constraints. *J. Water Resour. Plan. Manag.* **147**, 04021063 (2021).
37. Catalão, J. P. S., Mariano, S., Mendes, V. M. F. & Ferreira, L. Scheduling of head-sensitive cascaded hydro systems: a nonlinear approach. *IEEE Trans. Power Syst.* **24**, 337–346 (2008).
38. Hu, Z. *Energy Storage for Power System Planning and Operation* (Wiley, 2020).
39. Zhuo, Z. et al. Cost increase in the electricity supply to achieve carbon neutrality in China. *Nat. Commun.* **13**, 3172 (2022).
40. Yang, K. et al. *China Power Statistics Yearbook 2021* (China Electricity Council, 2021).
41. *Statistics of Photovoltaic Power Generation in 2018* (National Energy Administration, 2022); http://www.nea.gov.cn/2019-03/19/c_137907428.htm
42. *National Nuclear Power Operation from January to December 2018* (China Nuclear Energy Association, 2019); http://china-nea.cn/site/content/35592.html
43. Jekel, C. F. & Venter, G. pwlf: a Python library for fitting 1D continuous piecewise linear functions. https://github.com/cjekel/piecewise_linear_fit_py (2019).
44. *Global Coal Plant Tracker* (Global Energy Monitor, 2022); https://globalenergymonitor.org/projects/global-coal-plant-tracker/
45. Company profile. *China Southern Power Grid* http://eng.csg.cn/About_us/About_CSG/201601/t20160123_132060.html (2022).
46. Hu, Z., Tan, X. & Xu, Z. *An Exploration into China's Economic Development and Electricity Demand by the Year 2050* (Elsevier, 2013).
47. Chen, X. et al. Pathway toward carbon-neutral electrical systems in China by mid-century with negative CO_2 abatement costs informed by high-resolution modeling. *Joule* **5**, 2715–2741 (2021).
48. Minnaar, A. Time series classification and clustering. *Github* https://github.com/alexminnaar/time-series-classification-and-clustering (2016).
49. Gelaro, R. et al. The Modern-Era Retrospective Analysis for Research and Applications, version 2 (MERRA-2). *J. Clim.* **30**, 5419–5454 (2017).
50. Yaozhou, Z. & Bingcai, W. Pricing Irrigation Water in China. In Pricing Irrigation Water: Principles and Cases from Developing Countries (eds Tsur, Y. et al.) 198–215 (Resources for the Future Press, 2003).

Acknowledgements

This work was supported by Singapore's Ministry of Education (MOE) Academic Research Fund Tier-1 (A-0009297-01-00 and A-8000190-00-00). X.H. acknowledges the National University of Singapore's College of Design and Engineering for providing additional financial support through Outstanding Early Career Awards (A-8001228-00-00, A-8001389-00-00 and A-8001389-01-00). The computational work for this study was (fully/partially) performed using the resources of the National Supercomputing Centre, Singapore.

Author contributions

X.H. conceived the research. Z.L. performed the research and prepared the figures. Z.L. and X.H. analysed the results and wrote the paper.

Competing interests
The authors declare no competing interests.

Additional information
Extended data is available for this paper at https://doi.org/10.1038/s44221-023-00126-0.

Supplementary information The online version contains supplementary material available at https://doi.org/10.1038/s44221-023-00126-0.

Correspondence and requests for materials should be addressed to Xiaogang He.

Peer review information *Nature Water* thanks Sebastian Sterl and the other, anonymous, reviewer(s) for their contribution to the peer review of this work.

nature portfolio

Corresponding author(s): Xiaogang He

Last updated by author(s): Dec 7, 2022

Reporting Summary

Nature Portfolio wishes to improve the reproducibility of the work that we publish. This form provides structure for consistency and transparency in reporting. For further information on Nature Portfolio policies, see our Editorial Policies and the Editorial Policy Checklist.

Statistics

For all statistical analyses, confirm that the following items are present in the figure legend, table legend, main text, or Methods section.

n/a	Confirmed	
☐	☒	The exact sample size (*n*) for each experimental group/condition, given as a discrete number and unit of measurement
☒	☐	A statement on whether measurements were taken from distinct samples or whether the same sample was measured repeatedly
☒	☐	The statistical test(s) used AND whether they are one- or two-sided *Only common tests should be described solely by name; describe more complex techniques in the Methods section.*
☐	☒	A description of all covariates tested
☐	☒	A description of any assumptions or corrections, such as tests of normality and adjustment for multiple comparisons
☐	☒	A full description of the statistical parameters including central tendency (e.g. means) or other basic estimates (e.g. regression coefficient) AND variation (e.g. standard deviation) or associated estimates of uncertainty (e.g. confidence intervals)
☒	☐	For null hypothesis testing, the test statistic (e.g. *F*, *t*, *r*) with confidence intervals, effect sizes, degrees of freedom and *P* value noted *Give P values as exact values whenever suitable.*
☒	☐	For Bayesian analysis, information on the choice of priors and Markov chain Monte Carlo settings
☒	☐	For hierarchical and complex designs, identification of the appropriate level for tests and full reporting of outcomes
☒	☐	Estimates of effect sizes (e.g. Cohen's *d*, Pearson's *r*), indicating how they were calculated

Our web collection on statistics for biologists contains articles on many of the points above.

Software and code

Policy information about availability of computer code

Data collection	All data are collected based on Python scripts instead of specific software. A large part of the collected data has been provided in the Supplementary Information along with the paper. MERRA-2 data can be downloaded from https://disc.gsfc.nasa.gov/datasets?project=MERRA-2. Capacity factors of wind and solar power are calculated based on Python scripts (https://github.com/LDuan3008/Create_Wind_and_Solar_Resource_Files).
Data analysis	The energy expansion model PREP-SHOT is available under the GNU General Public License version 3 (GPLv3) and can be downloaded from the GitHub repo (https://github.com/PREP-NexT/PREP-SHOT) of the PREP-NexT (Pathways for REsilient Planning of water-energy-food Nexus Transformation) Lab, which is developed based on Python 3.8.0 and Pyomo 5.7.3. All models is solved by Gurobi 9.5.0.

For manuscripts utilizing custom algorithms or software that are central to the research but not yet described in published literature, software must be made available to editors and reviewers. We strongly encourage code deposition in a community repository (e.g. GitHub). See the Nature Portfolio guidelines for submitting code & software for further information.

Data

Policy information about availability of data

All manuscripts must include a data availability statement. This statement should provide the following information, where applicable:

- Accession codes, unique identifiers, or web links for publicly available datasets
- A description of any restrictions on data availability
- For clinical datasets or third party data, please ensure that the statement adheres to our policy

MERRA-2 data can be downloaded from https://disc.gsfc.nasa.gov/datasets?project=MERRA-2. All other data used in the optimization are provided in the Supplementary Information and cited from publicly available sources.

Human research participants

Policy information about studies involving human research participants and Sex and Gender in Research.

Reporting on sex and gender	NA
Population characteristics	NA
Recruitment	NA
Ethics oversight	NA

Note that full information on the approval of the study protocol must also be provided in the manuscript.

Field-specific reporting

Please select the one below that is the best fit for your research. If you are not sure, read the appropriate sections before making your selection.

☐ Life sciences ☐ Behavioural & social sciences ☒ Ecological, evolutionary & environmental sciences

For a reference copy of the document with all sections, see nature.com/documents/nr-reporting-summary-flat.pdf

Ecological, evolutionary & environmental sciences study design

All studies must disclose on these points even when the disclosure is negative.

Study description	This study develops a fully coupled reservoir operation and energy expansion model to quantify the economic and environmental benefits attained from flexible hydropower in a high-variable renewable energy (VRE) future.
Research sample	Our study considers existing 46 large hydropower stations with each installed capacity larger than 300MW in China Southern regional grid.
Sampling strategy	NA
Data collection	Key data/parameters are collected from existing literature and open source data platforms. MERRA-2 data can be downloaded from https://disc.gsfc.nasa.gov/datasets?project=MERRA-2. All other data used for optimization are provided in the Supplementary Information.
Timing and spatial scale	The hourly MERRA-2 reanalysis data (including surface incoming shortwave radiation, top of the atmosphere income shortwave radiation and 2-meter temperature, 10- and 50-meter wind speed) range from 1980-01-01 00:00:00 to 2019-12-31 23:00:00 and the spatial resolution is 0.625 degree (longitude) by 0.5 degree (latitude).
Data exclusions	No data were excluded from the analyses.
Reproducibility	Results can be reproduced using the developed tool (PREP-SHOT) and the datasets in GitHub repo.
Randomization	NA
Blinding	NA

Did the study involve field work? ☐ Yes ☒ No

Reporting for specific materials, systems and methods

We require information from authors about some types of materials, experimental systems and methods used in many studies. Here, indicate whether each material, system or method listed is relevant to your study. If you are not sure if a list item applies to your research, read the appropriate section before selecting a response.

Materials & experimental systems

n/a	Involved in the study
☒	☐ Antibodies
☒	☐ Eukaryotic cell lines
☒	☐ Palaeontology and archaeology
☒	☐ Animals and other organisms
☒	☐ Clinical data
☒	☐ Dual use research of concern

Methods

n/a	Involved in the study
☒	☐ ChIP-seq
☒	☐ Flow cytometry
☒	☐ MRI-based neuroimaging